Planar second-harmonic generation with noncollinear pumps in disordered media

Vito Roppo[1], David Dumay[2], Jose Trull[1], Crina Cojocaru[1], Solomon M. Saltiel[2,3], Kestutis Staliunas[1], Ramon Vilaseca[1], Dragomir N. Neshev[2], Wieslaw Krolikowski[2], and Yuri S. Kivshar[2]

[1]*Departament de Fisica i Enginyeria Nuclear, Escola Técnica Superior d'Enginyeries Industrial y Aeronáutica de Terrassa, Universitat Politécnica de Catalunya, 08222 Terrassa, Barcelona, Spain*

[2]*Nonlinear Physics Center and Laser Physics Center, Center for Ultrahigh Bandwidth Devices for Optical Systems (CUDOS), Research School of Physical Sciences and Engineering, Australian National University, Canberra ACT 0200, Australia*

[3]*Faculty of Physics, University of Sofia, 5 J. Bourchier Boulevard, BG-1164, Sofia, Bulgaria*

Abstract: We study experimentally the process of the second harmonic generation by two noncollinear beams in quadratic nonlinear crystals with a disordered structure of ferroelectric domains. We show that the second-harmonic radiation is emitted in the form of two cones as well as in a plane representing the cross-correlation of the two fundamental pulses. We demonstrate the implementation of this parametric process for characterisation of femtosecond pulses, enabling the estimation of pulse width, chirp, and front tilt. This is achieved through monitoring the evolution of the autocorrelation trace inside the nonlinear crystal.

OCIS codes: (190.0190) Nonlinear optics; (190.4420) Nonlinear optics: Nonlinear optics, transverse effects in.

References and links

1. M. Horowitz, A. Bekker, and B. Fischer, "Broadband second-harmonic generation in $SrBaNb_2O_6$ by spread spectrum phase matching with controllable domain gratings," Appl. Phys. Lett. **62,** 2619–2621 (1993).
2. J. J. Romero, C. Arago, J. A. Gonzalo, D. Jaque, and J. Garcia Sole, "Spectral and thermal properties of quasi-phase-matchingsecond-harmonic generation in Nd^{3+}:$Sr_{0.6}Ba_{0.4}(NbO_3)_2$ multi-self-frequency-converter nonlinear crystals," J. Appl. Phys. **93,** 3111–3113 (2003).
3. R. Fischer, D. N. Neshev, S. Saltiel, W. Krolikowski, and Yu. S. Kivshar, "Broadband femtosecond frequency doubling in random media," Appl. Phys. Lett. **89,** 191105 (2006).
4. P. Molina, M. O. Ramirez, and L. E. Bausa, "Strontium Barium Niobate as a Multifunctional Two-Dimensional Nonlinear "Photonic Glass,"" Adv. Funct. Mat. **18,** 709–715 (2008).
5. M. O. Ramirez, D. Jaque, L. Ivleva, and L. E. Bausa, "Evaluation of ytterbium doped strontium barium niobate as a potential tunable laser crystal in the visible," J. Appl. Phys. **95**, 6185–6191 (2004).
6. A. R. Tunyagi, M. Ulex, and K. Betzler, "Noncollinear optical frequency doubling in strontium barium niobate," Phys. Rev. Lett. **90,** 243901 (2003).
7. A. R. Tunyagi, "Non-Collinear Second Harmonic Generation in Strontium Barium Niobate," PhD thesis, Fachbereich Physik, Universität Osnabrück, Germany (2004).
8. R. Fischer, D. N. Neshev, S. M. Saltiel, A. A. Sukhorukov, W. Krolikowski, and Yu. S. Kivshar, "Monitoring ultrashort pulses by transverse frequency doubling of counterpropagating pulses in random media," Appl. Phys. Lett. **91,** 031104 (2007).
9. S. M. Saltiel, D. N. Neshev, R. Fischer, A. Arie, W. Krolikowski, and Yu. S. Kivshar, "Spatiotemporal toroidal waves from the transverse second-harmonic generation," Opt. Lett. **33,** 527–529 (2008).
10. J. Janszky, G. Corradi, and R. N. Gyuzalian, "On a possibility of analysing the temporal characteristics of short pulses," Opt. Commum. **23,** 293–298 (1977).
11. S. M. Saltiel, S. D. Savov, I. V. Tomov, and L. S. Telegin, "Subnanosecond pulse duration measurements by noncollinear second harmonic generation," Opt. Commun. **38,** 443–447 (1981).

#99821 - $15.00 USD Received 6 Aug 2008; revised 21 Aug 2008; accepted 21 Aug 2008; published 26 Aug 2008

12. Y. Ishida, T. Yajima, and A. Watanabe, "A simple monitoring system for single subpicosecond laser pulses," Opt. Commun. **56,** 57–60 (1985).
13. M. Baudrier-Raybaut, R. Haidar, Ph. Kupecek, Ph. Lemasson, and E. Rosencher, "Random quasi-phase-matching in bulk polycrystalline isotropic nonlinear materials," Nature (London) **432,** 374–376 (2004).
14. J. Trull, C. Cojocaru, R. Fischer, S. Saltiel, K. Staliunas, R. Herrero, R. Vilaseca, D. N Neshev, W. Krolikowski, and Yu. S. Kivshar, "Second-harmonic parametric scattering in ferroelectric crystals with disordered nonlinear domain structures," Opt. Express **15,** 15868–15877 (2007).
15. G. Agrawal, *Nonlinear Fiber Optics*, Ch. 3, (Academic Press, 2007).
16. S. Akturk, M. Kimmel, P. O'Shea, and R. Trebino "Measuring pulse-front tilt in ultrashort pulses using GRENOUILLE," Opt. Express **11,** 491–501 (2003).

1. Introduction

Recently, it was demonstrated that quadratic nonlinear crystals consisting of antiparallel ferroelectric domains with randomized sizes and positions can be employed for the phase-matched second-harmonic generation (SHG) in a wide spectral range of the crystal transparency window without a need of angle alignments or temperature tunings (see, e.g. Refs. [1, 2, 3, 4] and references therein). Such a disordered nonlinear medium has a great advantage over other types of quadratic media where the phase-matching conditions require either birefringence or engineered periodical poling of the nonlinear quadratic medium. The frequency-independent phase matching in the unpoled crystals is known to occur due to randomness in the size and distribution of the antiparallel ferroelectric domains. The needle-like ferroelectric domains are orientated along the Z-axis (c-axis) of the crystal, and thus they create an effective two-dimensional nonlinear photonic structure (2DNPS) with a constant linear refractive index but randomly alternating sign of the nonlinear quadratic response. A prominent example of such nonlinear media is an unpoled crystal of Strontium Barium Niobate (SBN). The diameter of its domains varies typically between 1 μm and 8 μm [2], and it can even reach the sub-micron dimensions [4, 5]. Such disordered 2DNPS can be considered as being composed of an infinite number of $\chi^{(2)}$ gratings where the corresponding reciprocal vectors have random magnitudes and orientations in the X-Y (a-b) plane. In this way, an infinite number of reciprocal vectors is available to realize different types of the phase matching conditions. It has been demonstrated recently that depending on geometry of interaction the second-harmonic (SH) radiation can be generated either in the form of a cone [3, 4, 6] or in a plane [3, 4] depending on whether the fundamental wave propagates along or perpendicular to the c-axis of the crystal, respectively. The planar emission of the SH waves occurs with almost equal efficiency in both forward and transverse directions. For any other propagation direction of the fundamental beam (except for the direction perpendicular to Z) the generated SH wave is emitted in the form of a cone. The bigger the deviation from axis Z is, the bigger is the cone angle [3, 7].

In this paper, we study noncollinear interaction of short optical pulses in a SBN crystal with disordered domain structure by using two fundamental waves intersecting inside the crystal. We demonstrate that these two waves can generate a SH wave in a plane. We investigate the spatial structure of the transversely generated SH radiation along the propagation direction and show that this effect may be employed as a simple tool for monitoring both the structure and evolution of short pulses in nonlinear media.

2. Phase-matching conditions and parameters of the SH emission

2.1. Phase-matching conditions

In our earlier papers on parametric processes in unpoled SBN crystals, we considered mainly collinear pump interaction schemes [3, 8, 9]. For a single fundamental beam propagating along or perpendicular to the optical axis (which coincides with the domain orientation) the phase-matching condition results in SH radiation emitted in a form of a cone or a plane.For counter-

#99821 - $15.00 USD Received 6 Aug 2008; revised 21 Aug 2008; accepted 21 Aug 2008; published 26 Aug 2008

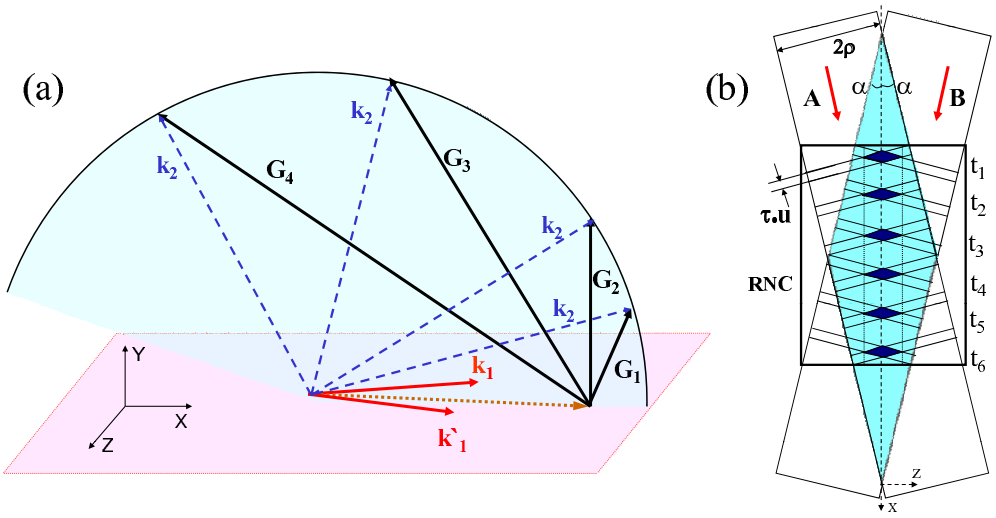

Fig. 1. (a) Schematic of the phase-matching diagram demonstrating the planar emission of the SH wave via interaction of two noncollinear pumps with bisector coinciding with crystal axis X. $\mathbf{G}_i$ being the reciprocal vectors of the disordered nonlinear crystal. (b) Overlap of the beams **A** and **B** and the overlap of the short pulses forming a narrow line inside the crystal.

propagating pumps being either perpendicular to [8] or directed along the z-axis [9] the SH signal is also emitted in a form of a plane.

Here, we consider two fundamental beams propagating in crystallographic plane $X-Z$ of the SBN crystal and forming angles $-\alpha$ and $+\alpha$ with the X axis. Then the general vectorial phase-matching condition for SHG is written as $\mathbf{k}_2 = \mathbf{k}_1^{'} + \mathbf{k}_1 + \mathbf{G}$, where $\mathbf{k}_1, \mathbf{k}_1^{'}$ and $\mathbf{k}_2$ are the wave vectors of the fundamental and second-harmonic waves, respectively, and **G** represents one of the reciprocal vectors available from the infinite set of vectors provided by a disordered nonlinear photonic structure. The phase-matching conditions that require three-dimensional consideration are visualized in Fig. 1(a). The blue arc defines the geometrical place of the $\mathbf{k}_2$ direction. All reciprocal vectors **G** are situated in the $X-Y$ plane. Taking into account that these vectors can take any length and direction within this plane, we notice that all possible phase-matching triangles determine that the SH radiation is emitted in the form of a plane coinciding with the crystal $X-Y$ plane.

2.2. Parameters of the SH emission

Because the SH signal is generated in the area where the pulses from each fundamental beam overlap, the width of the emission region is directly related to the pulse length and beam size [see Fig. 1(b)]. Let us consider two distinct limiting cases: (i) interaction of *long pulses*, when the pulse width $\tau \gg 2\rho \tan\alpha/u$, where α is the angle between each of the beams and the crystal axis X, ρ is the beam radius, and u is the speed of light in the crystal; and (ii) interaction of *short pulses* when $\tau \ll 2\rho \tan\alpha/u$. In the case (i), the SH radiation is generated from the volume overlap of the two fundamental beams and the width of the emission area Δz is defined as $\Delta z = 2\rho/\cos\alpha$. In the second case (ii), the SH emission area is defined by the temporal overlap of both pulses and has form of a thick line with the width of $\Delta z = \tau u/\sin\alpha$. This relation is valid for identical rectangular pulses with the duration τ. In the case of Gaussian

#99821 - $15.00 USD Received 6 Aug 2008; revised 21 Aug 2008; accepted 21 Aug 2008; published 26 Aug 2008

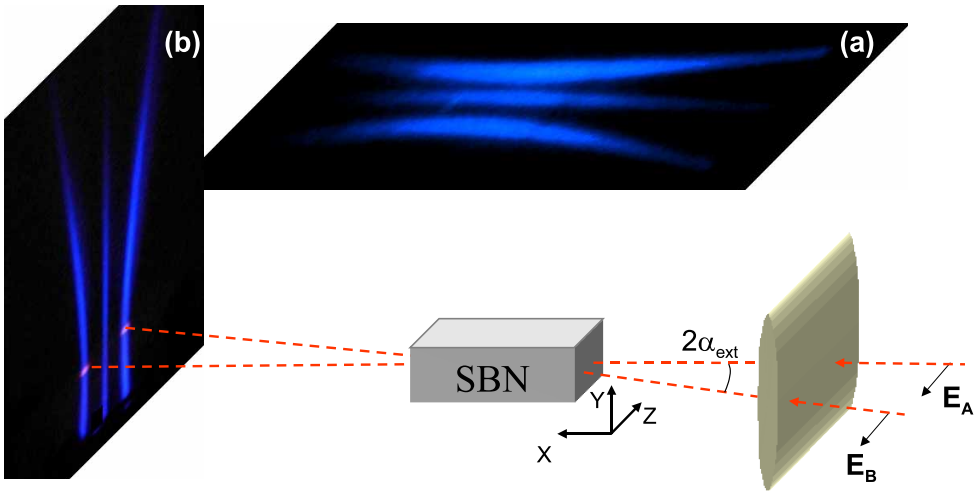

Fig. 2. Photographic images of the SH emission in the transverse (a) and forward (b) directions via noncollinear waves interaction. The middle line in both photos corresponds to the planar SH emission as a result of the mixing of the two beams/pulses A and B ($\lambda = 810$ nm). These central traces disappear if one of the input beams (A or B) is blocked or if the pulses do not overlap inside the crystal. The two arcs on both sides of the central lines represent the conical emission from each individual pump beam [3, 4, 6]. Media 1 shows images recorded in forward direction: right beam (A) blocked; left beam (B) blocked; both beams ON - big delay between the femtosecond pulses; both beams ON - no delay between the femtosecond pulses.

pulses, the width of the SH emission area will be $\sqrt{2}$ smaller [10]

$$\Delta z = \tau u/(\sqrt{2}\sin\alpha), \tag{1}$$

leading to following relation $\tau = \Delta z\sqrt{2}\sin\alpha/u$. This is the well-known formula for the pulse duration single-shot measurements by noncollinear SHG experiments, see e.g. Refs. [10, 11, 12]. The difference is that in the traditional pulse-duration measurement techniques the recording of the SH trace is performed in forward direction, integrated over the crystal length. This is due to the fact that the phase-matching conditions are only fulfilled in the forward direction. In the situation considered here, we deal with an emission also in the transverse direction, due to the specific for this type of media all-directions *random quasi phase matching* [13]. Therefore, the two-pulse overlapping volume is moving towards the output face, resulting in a SH line as illustrated in Fig. 1(b). Monitoring transversely the width of this line along the crystal length can now provide an additional information about the pulse evolution inside the SH crystal.

3. Experimental results and discussion

Two types of experiments have been conducted by using light sources with different wavelengths and pulse durations. In the first experiment, the fundamental waves are generated by a femtosecond MIRA (Coherent) oscillator tuned to 810 nm, with the pulse duration $\tau = 180$ fs and repetition rate 76 MHz. In the second experiment, we use a Nd:YAG laser [14] delivering 8 ns pulses at 1064 nm wavelength with repetition rate of 10 Hz.

The schematic representation of the experimental geometry is displayed in Fig. 2. The incoming infrared laser beam is split into two equal parts (with the amplitudes E_A and E_B) which are incident at an unpoled SBN crystal ($5\times5\times10$ mm, all sides polished) under an acute angle

#99821 - $15.00 USD Received 6 Aug 2008; revised 21 Aug 2008; accepted 21 Aug 2008; published 26 Aug 2008

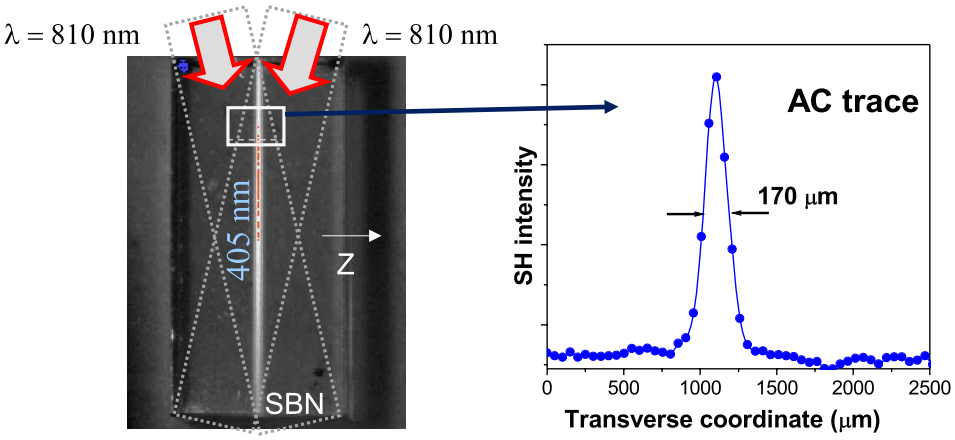

Fig. 3. Left: The AC trace of transversely emitted SHG from two intersecting fundamental beams. The movie Media 2 associated with this photo shows the change of the position of the AC trace with variation of the delay between the pulses. Each step corresponds to 104 fs delay. Right: Detailed profile of the AC trace.

such that the two beams intersect in the central part of the crystal. The externally measured intersection angle $2\alpha_{\text{ext}}$ in different measurements is in the range of $20^\circ - 28^\circ$. We note that it is essential to have a large beam width in the plane of the crossing angle in order to fulfil the requirement for *short pulse* nonlinear interaction discussed above. For this reason, the beams are focused in the crystal with a cylindrical lens ($f = 10$ cm), resulting in beam transverse dimension in the range of 2.2 mm$\times$0.43 mm. The path lengths of both incident beams are adjusted to ensure that the propagating pulses meet inside the crystal.

In the experiments, the polarization vectors of both pump beams are chosen to be extraordinary, being directed along the crystallographic axis Z. The generated SH radiation is also polarized along Z indicating the interaction of the type $e_A e_B - e_{SH}$. This interaction gives the highest efficiency compared with other two possible geometries, namely $o_A o_B - e_{SH}$ and $o_A e_B - o_{SH}$. In this notation, 'e' means an extraordinary wave and 'o' – an ordinary wave. The 4mm point symmetry group of the SBN crystal determines nonzero components of the second-order nonlinearity tensor $\hat{d}^{(2)}$. Since the direction of the fundamental beams is close to or coincides with the crystallographic axis X, the relevant $\chi^{(2)}$ component for $e_A e_B - e_{SH}$ is d_{33}.

The photos in Fig. 2 illustrate experimentally observed (a) transversely and (b) forward emitted SH signal for the noncollinear interaction of the fundamental beams in the SBN crystal. In each photograph, the central line appears only if two femtosecond pulses overlap inside the crystal. Blocking one of the beams or introducing a relatively large delay (> 2 ps) for one of the pulses makes this line to disappear. The two arcs located symmetrically on each side of the central trace represent the conical emissions from each individual pump beam [3, 4, 6]. They are formed as a result of the collinear interaction of the fundamental photons within each beam. The internal cone angle β is defined by the phase-matching conditions similar to that discussed in Refs. [3, 6] but modified to account for an arbitrary position of the fundamental beam with respect to the X axis. Actually, the cone angle β can be found from the relation [3, 7]

$$\beta = \cos^{-1}[(2k_1/k_2)\sin\alpha]. \tag{2}$$

Based on the internal angle α corresponding to the present experiment, we obtain that the external cone angle $\beta_{\text{ext}} = 79^\circ$.

#99821 - $15.00 USD Received 6 Aug 2008; revised 21 Aug 2008; accepted 21 Aug 2008; published 26 Aug 2008

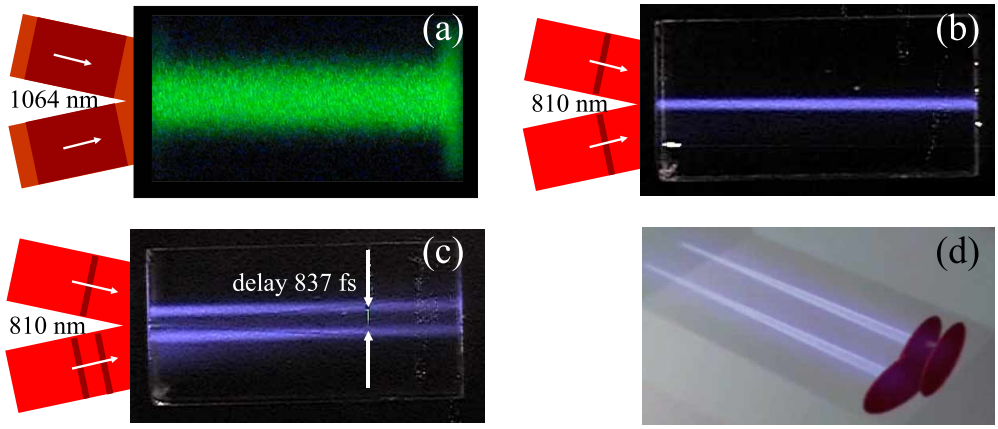

Fig. 4. (a-b) Comparison of the thicknesses of the planar SH emission in the case of (a) nanosecond and (b) femtosecond pulses; (c) cross-correlation of a single and double femtosecond pulses. The delay between two constituent pulses in the doublet is 837 fs. (d) The Media 3 illustrates schematically the formation of AC trace, cross-correlation trace, and pulse-front tilt.

The transverse distribution of the middle trace inside the crystal represents the autocorrelation (AC) signal of the incoming femtosecond pulses [10]. It is important to note that the SH signals from the fundamental beams are emitted conically and propagate at different angles. Therefore they do not interfere with the correlation signal, rendering it background-free.

Figure 3 shows the AC trace measured for the case of 810 nm fundamental waves. As both pulses enter the crystal simultaneously, the trace is located centrally inside the geometrical region of an overlap of both incoming beams. The plot on the right depicts a detailed profile of the AC trace. In the presence of a temporal delay between the fundamental pulses, the AC line will shift transversely to left or right by $\delta z = u\delta t/2\sin\alpha$, as illustrated by the movie associated with this figure. This lateral shift can be used to calibrate the AC measurements. On the right hand side of Fig. 3, a digitized trace from the region close to the entrance side of the crystal is shown. According to Eq. (1), its width gives the FWHM pulse duration of 193 fs .

In Figs. 4(a-b) we demonstrate the dependence of the width of the planar SH emission on the pulse duration. For long (8 ns) pulses [Fig. 4(a)] the trace fills the entire overlapping area of the beams. In this particular experiment the intersection angle $2\alpha_{\text{ext}} \approx 22^0$. On the other hand, in the case of femtosecond pulses [see Fig. 4(b)] the trace has a form of a narrow line located inside the area of an overlap of both beams. In this case, the thickness of the trace directly reflects the pulse duration, with intensity distribution representing the AC function of the pulses. Figure 4(c) illustrates the cross-correlation signal obtained when one of the beams contains a sequence of two pulses separated by a delay of 837 fs. This pulse doublet is obtained by splitting the original femtosecond pulse utilizing the difference in the velocities of the orthogonally polarized pulses in a birefringent lithium niobate crystal [8]. As a result, the correlation trace has a form of two parallel lines. The movie accompanying Fig. 4(d) illustrates schematically the formation of an AC trace, cross-correlation trace, and pulse front tilt.

Another attractive feature of the transverse recording of the AC traces is a possibility to monitor the evolution of the pulses during their propagation in the SH crystal. This evolution provides important additional information for the initial chirp of the pulses. Indeed, our experimental results [Fig. 5(left)] clearly show that the width of the AC trace increases with the propagation distance. This monotonic broadening of the AC trace reflects an accumulation of a

#99821 - $15.00 USD Received 6 Aug 2008; revised 21 Aug 2008; accepted 21 Aug 2008; published 26 Aug 2008

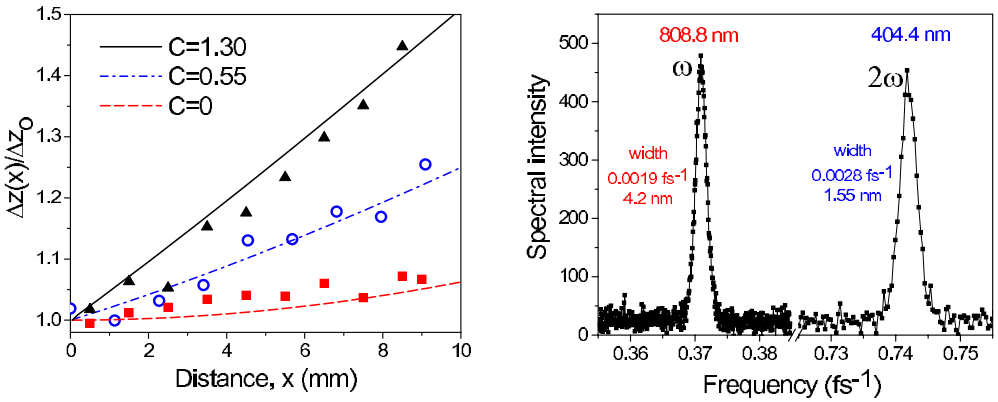

Fig. 5. Left: Increase of the FWHM width of the AC trace as a function of the distance from the input face of the SBN crystal for three different alignments of the femtosecond laser. The lines represent the predicted AC trace broadening for the cases without input chirp, with a linear input chirp of $C = 0.55$, and with a linear input chirp of $C = 1.3$. Right: Measured spectra of the fundamental and SH signals.

pulse chirp during the propagation in the dispersive SBN crystal, as well as a possible existence of an initial pulse chirp. Assuming that the pulse propagating inside the crystal is not modified by nonlinear effects (being only affected by the group-velocity dispersion of the SBN crystal), we can estimate the value of the input pulse chirp by measuring the pulse broadening. In order to check if the pulse evolution inside the SBN crystal is indeed not affected by possible third-order nonlinear effects, we compare the spectra of the fundamental and SH beams [Fig. 5(right)]. We see that the fundamental spectrum is not distorted, and the SH spectrum is exactly $\sqrt{2}$ broader, as should be expected for the SHG process without depletion and group-velocity mismatch.

The results in Fig. 5(left) illustrate the broadening of the AC trace for three different alignments of the laser. Note that, despite the identical initial AC width in all three cases, the rate of its expansion varies significantly. In order to explain this behaviour, we took into account a possible initial linear chirp. In this case, we theoretically calculate the broadening of the AC trace, $\Delta z(x)$ as follows,

$$\Delta z(x)/\Delta z_0 = \tau_{\text{chirp}}(x)/\tau_0, \tag{3}$$

where Δz_0 is the AC trace width close to the input face, and τ_{chirp} is the dispersion-induced broadening of the femtosecond pulse duration, assuming Gaussian pulse profile [15]

$$\tau_{\text{chirp}}(x) = \tau_0\sqrt{(1+4\ln 2C\beta_2 x/\tau_0^2)^2 + (4\ln 2\beta_2 x/\tau_0^2)^2}, \tag{4}$$

with parameter C representing an initial chirp. The results of calculations using the above formula are depicted as solid, dashed and dash-dotted lines in Fig. 5. Very good agreement between theory and experimental data is obtained assuming linear chirp of $C = 0$, $C = 0.55$ and $C = 1.3$, for the three lines respectively. In these calculations we also assumed that $\beta_2(\text{SBN}) = -466\ \text{fs}^2/\text{mm}$ and $\tau_0 = 190\ fs$ (FWHM).

This result demonstrates the applicability of the experiments in random nonlinear media to monitor not only the pulse duration, but also the presence of an input chirp through monitoring the evolution of femtosecond pulses inside the SH crystal. In addition, the scheme can directly visualize in the transverse direction the pulse front tilt [see movie in Fig. 4]. In this case, the AC trace will not coincide with the crystal X axis but will be tilted at an angle directly related to the pulse front tilt [16].

#99821 - $15.00 USD Received 6 Aug 2008; revised 21 Aug 2008; accepted 21 Aug 2008; published 26 Aug 2008

4. Conclusions

We have studied the second-harmonic generation by noncollinear fundamental beams in a nonlinear quadratic crystal with disordered distribution of ferroelectric domains. While the overall efficiency of this parametric process is low, this effect allows us to realize a simple femtosecond pulse monitoring system. This system is achromatic, it does not require angle or temperature tuning, and it enables observation of the pulse evolution during its propagation in the crystal.

Acknowledgments

The authors from Universitat Politécnica de Catalunya thank Ministerio de Educacion y Ciencia for the financial support through Project FIS2005-07931-C03-03. The researchers in Australia acknowledge a support of the Australian Research Council. All authors acknowledge also the support of COST MP0702 action. Solomon Saltiel thanks the Australian National University and Universitat Politécnica de Catalunya for hospitality and support. The authors thank Dr. Vesselin Kolev for his help with the experiments.

#99821 - $15.00 USD Received 6 Aug 2008; revised 21 Aug 2008; accepted 21 Aug 2008; published 26 Aug 2008